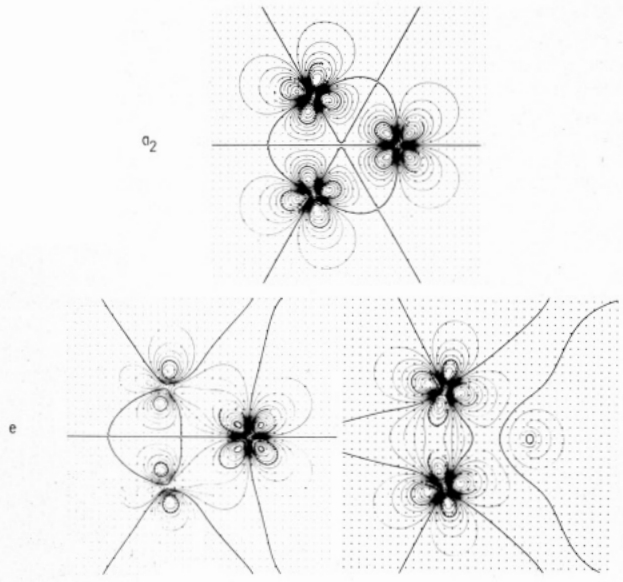


Figure 7. Contour diagram, in the triangular metal plane, of the three important Co_3 orbitals in $[Co(C_5H_5)]_3(S)(NH)$.

e orbitals consist of Cp (ca. 44%), Co (ca. 42%), and capping ligand (14%) contributions.

Construction of these a_2 and e orbitals from the corresponding orbitals of the metal-triangle fragment and a pair of capping ligands is shown in Scheme I. Since the a_2 orbital of the metal fragment cannot interact with the orbitals of the capping ligands because of the symmetries, its energy level remains unchanged on construction of the final complex. In contrast, the degenerate e orbitals of the metal fragment interact rather effectively with the $p\pi$ orbitals of the capping ligands, the repulsive part of which gives HOMOs for the total complex in the case of **5** and **6**. In the case of **7**, however, the same interaction results in LUMOs for the total complex since the a_2 orbital now lies at lower energy level and takes up the two electrons (Scheme I).

The origin of this different order of the a_2 and e orbitals with the change of the capping ligands can be traced back to the different sizes of the triangular metal frames, the largest in **7** and the smallest in **5**, which in turn are governed by sizes of the capping ligands (see the X-ray section). The metal–metal distances used in the present calculations were 2.42 Å for **5**, 2.578 Å for **6**, and 2.688 Å for **7**. In accordance with the orbital character shown in Figure 7, the a_2 orbital of the metal fragment stabilizes and the e orbitals slightly destabilize with the increase of the metal–metal distances (Scheme I). Consequently, the energy difference between these two orbital levels of the metal fragment is maximum in **5** and minimum in **7**. In complex **7**, good overlap of the sulfur $3p\pi$ orbitals with the e orbitals of the metal fragment raises these orbitals to the level higher than that of the relatively low-lying a_2 orbital.

Although the metal core of **1** in the solid state is frozen in a distorted form by crystal packing forces, it could be relaxed in solution to a configuration close to that of an equilateral metal triangle because its thermodynamically stable isomer in solution at low temperatures is the triplet isomer. As the rotational barrier of a coordinated cyclopentadienyl ring is very small,[20] independent rotational motion of the three ZCp rings in solution would break the 3-fold symmetry only very weakly. On the basis of the MO analysis, the triplet-state orbital configuration of **1** is expected to be $e^2a_2^0$ and that for **2** to be $a_2^1e^1$. The different orbital configuration of the triplet state may be responsible for the different paramagnetic NMR frequency shifts of the ZCp ligands in **1** and **2**; viz., resonances of the ring protons are resolved in **2** but not in **1** and the methyl and ring protons shift in the same direction in **1** but shift in opposite directions in **2**.

Supplementary Material Available: Lists of anisotropic thermal parameters for non-hydrogen atoms and positional and isotropic thermal parameters for hydrogens (3 pages); a list of calculated and observed structure factors (19 pages). Ordering information is given on any current masthead page.

(20) Aleksandrov, A.; Struckhov, Yu. T.; Khandkarova, V. S.; Gubin, S. P. *J. Organomet. Chem.* **1970**, *25*, 243.

Contribution from the Department of Chemistry, University of Delaware, Newark, Delaware 19716

Synthesis and Modes of Coordination of Energetic Nitramine Ligands in Copper(II), Nickel(II), and Palladium(II) Complexes

S. F. Palopoli, S. J. Geib, A. L. Rheingold, and T. B. Brill*

Received February 3, 1988

New Cu(II), Ni(II), and Pd(II) complexes of nitraminato ligands derived from methylnitramine, ethylenedinitramine, and a nitroaminotetrazole are reported. A wide variety of modes of metal–ligand coordination have been uncovered by X-ray crystallography. The nitraminato ligands are able to bond through the O or the N donor sites alone or chelate by coordination at both the O and N sites. N,N′-Chelate complexes, bridging nitraminato ligands leading to dimers, and crystalline polymers have also been produced. Crystal data: for *trans*-$[Cu(NH_3)_2\{N(NO_2)CH_3\}_2]$, monoclinic, $P2_1/c$, a = 7.3786 (8) Å, b = 6.2543 (8) Å, c = 10.123 (2) Å, β = 102.00 (1)°, V = 457.0 (1) Å^3, Z = 2; for $[Cu(en)\{N(NO_2)CH_3\}_2]$, monoclinic, $P2_1/c$, a = 12.282 (3) Å, b = 9.150 (2) Å, c = 10.563 (3) Å, β = 113.69 (2)°, V = 1087.0 (6) Å^3, Z = 4; for $[Cu(NH_3)_2\{N(NO_2)CH_2CH_2N(NO_2)\}]$, triclinic, $P\bar{1}$, a = 5.851 (2) Å, b = 6.392 (4) Å, c = 6.501 (3) Å, α = 97.24 (4)°, β = 108.02 (4)°, γ = 111.46 (4)°, V = 207.2 (2) Å^3, Z = 1; for β-$[Ni(H_2O)_4\{N(NO_2)CH_2CH_2N(NO_2)\}]$, monoclinic, $C2/c$, a = 12.584 (3) Å, b = 7.867 (2) Å, c = 10.627 (2) Å, β =111.18 (2)°, V = 980.9 (5) Å^3, Z = 4; for α-$[Ni(H_2O)_4\{N(NO_2)CH_2CH_2N(NO_2)\}]$, monoclinic, $P2_1/n$, a = 13.508 (2) Å, b = 11.166 (2) Å, c = 14.133 (2) Å, β = 114.23 (1)°, V = 1942.3 (5) Å^3, Z = 8; for $[Ni(NH_3)_3\overline{NNNNCNNO_2)}]_2$, monoclinic, $P2_1/n$, a = 7.200 (1) Å, b = 16.864 (3) Å, c = 7.349 (1) Å, β = 114.25 (2)°, V = 813.5 (3) Å^3, Z = 2; for $[Cu_2(en)_2\{N(NO_2)CH_2CH_2N(NO_2)\}_3]\cdot 2H_2O$, triclinic, $P\bar{1}$, a = 7.727 (5) Å, b = 10.248 (6) Å, c = 11.367 (7) Å, α = 90.90 (5)°, β = 108.26 (5)°, γ = 96.82 (5)°, V = 847.4 (9) Å^3, Z = 1.

Introduction

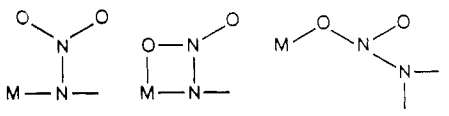
Many organic nitramines are well-known for their exothermic, autocatalytic thermal decomposition. Thus, they are of interest as rocket propellants and explosives. Concern about the amount of stored energy in these molecules may have inhibited investigations of their coordination tendencies despite the fact that selected nitramines would form an interesting class of ligands.[1-3] One unusual feature is that the atom geometry at the amine donor

(1) (a) Franchimont, A. P. N. *Rec. Trav. Chim. Pays-Bas* **1894**, *13*, 307. (b) Davis, T. L.; Ou, C. W. *J. Am. Chem. Soc.* **1934**, *56*, 1064. (c) Liebig, D. M.; Robertson, J. H. *J. Chem. Soc.* **1965**, 5801.

0020-1669/88/1327-2963$01.50/0 © 1988 American Chemical Society

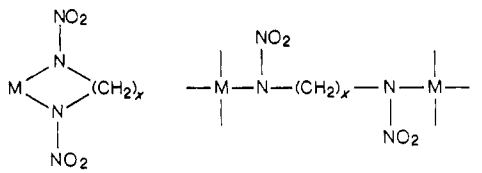
site is essentially constrained to a trigonal plane. Another feature of interest is that the nitramine might coordinate at the amine nitrogen atom, the oxygen atom, or both.

This paper describes the synthesis and structure of several nitraminato complexes of Cu(II) and Ni(II) and the synthesis of a Pd(II) complex. The crystal structure determinations in this work combined with two previously determined structures[1c,2] give a reasonably complete picture of the various modes of coordination possible for nitraminato ligands. The progression of bonding interaction from (strong) N–(weak) O (**1**) to (strong) N–(strong) O (**2**) to (strong) O–(no) N (**3**) is observed with the structures



1 **2** **3**

now available. For terminal dinitramines, both the chelate (**4**) and polymeric bridging (**5**) modes of coordinations are observed.



4, $x = 2, 3$ **5**, $x = 2, 4$

We investigated this subject in part because of the potential that metal–nitraminato complexes might be useful as burn-rate catalysts or ballistic modifiers toward organic nitramines. The burn-rate of nitramine-based propellants has been difficult to tailor.[4] We hoped that the nitraminato ligands would make these complexes compatible with the bulk nitramine and that, on decomposition, the heat release and the coordinative unsaturation at the metal center as the ligands leave might catalyze and accelerate the thermolysis reactions. In addition, ammonia is known to accelerate the rate of decomposition of nitramines.[4] Some of the complexes synthesized release NH_3 on thermolysis. The following paper in this issue describes the thermolysis properties of these complexes at high heating rates. As revealed in the results of that paper, these complexes appear to have positive heats of formation and indeed store considerable energy. With this in mind, they were synthesized in relatively small quantities and were handled with the precautions that should be accorded to any energetic material.

Experimental Section

Materials. 1,3-Dimethylurea, 2-imidazolidone, *n*-butyllithium (1.6 M/hexane), hydrazine hydrate (85%), nitroguanidine, *tert*-butylamine, and potassium nitrite were obtained from Aldrich. Copper(II) nitrate, nickel(II) nitrate, and potassium nitrate were purchased from Fisher Scientific (ACS Reagent Grade). Palladium(II) chloride was obtained from Johnson Matthey, Inc. Solvents were purchased from J. T. Baker or Fisher. Diethyl ether and hexane were dried by reflux and distillation over sodium/benzophenone for the *tert*-butylnitramine synthesis. Ethyl nitrate was provided by Dr. R. Willer of Morton-Thiokol, Inc. The ethyl nitrate was passed through an alumina column and dried over anhydrous magnesium sulfate prior to use. All other materials were used as received.

Ligand Synthesis. 100% nitric acid for the nitrations was prepared as follows: Glassware for the preparations was cleaned with aqua regia, rinsed with pure distilled water, and oven-dried prior to use. Fluorocarbon grease was used on the standard taper joints. To start, 600 g of dry potassium nitrate was added slowly, with mechanical stirring under a nitrogen purge, to 1000 mL of concentrated sulfuric acid in a three-neck flask cooled in an ice bath. The resulting mixture was distilled under vacuum with a minimum of heat. Colorless nitric acid was collected in a receiver immersed in a dry ice–isopropyl alcohol bath. The distillation was conveniently followed by monitoring the pot (mixture) temperature,[5] which initially rose slowly from about 0 °C to about ambient temperature. Near the end of the distillation the temperature rose rapidly. The distillation was terminated when a pot temperature of about 75 °C was reached. The 100% nitric acid was stored frozen (<–43 °C) in the dark for up to a week without significant autodecomposition.

Methylnitramine was prepared by nitration of 1,3-dimethylurea using the method of Manser.[6] Ethylenedinitramine (EDNA) was prepared by nitration of 2-imidazolidone.[7] Potassium 5-nitroamintetrazolate was synthesized by reaction of nitroaminoguanidine with potassium nitrate using the method of Henry et al.[8] Nitroaminoguanidine was prepared by hydrazinolysis of nitroguanidine.[9] *tert*-Butyl nitramine was prepared by conversion of *tert*-butylamine to its conjugate base using *n*-butyllithium, followed by nitration with ethyl nitrate.[10]

Metal Hydroxides. Copper and nickel hydroxide were prepared fresh from metal nitrate (5 mmol) solutions and excess sodium hydroxide (15 mmol) dissolved in about 20 mL of distilled water. For copper hydroxide the two solutions were cooled to 0 °C before mixing. The metal hydroxides were collected by filtration and thoroughly washed with distilled water.

Metal Complexes. Elemental analyses were obtained on all compounds and were good in all cases. The yield of each compound was not determined because no attempt was made to optimize it. However, the product described is the dominant one to crystallize based on the uniformity of the crystals and the mass of material produced. *Caution!* The complexes synthesized here explode upon hammer impact and on rapid heating on a hot plate.

Diamminebis(methylnitraminato)copper(II) (I). $Cu(NO_3)_2 \cdot 2.5H_2O$ (1.16 g, 5 mmol) and NH_4NO_3 (1.6 g, 20 mmol) were dissolved together in about 10 mL of distilled water. Sodium methylnitraminate (2.0 g, 20 mmol) dissolved in about 10 mL of distilled water was then added followed by the addition of 50 mL of methanol. After being stirred for 30 min, the solution was filtered and 50 mL of ethylacetate was added to the filtrate. The complex crystallized from the filtrate at 0 °C over a period of 2 weeks. I can also be prepared by the method used for II. However, diffraction quality crystals were not obtained by this latter method.

(Ethylenediamine)bis(methylnitraminato)copper(II) (II). $Cu(NO_3)_2 \cdot 2.5H_2O$ (1.16 g, 5 mmol) was dissolved in aqueous ammonium hydroxide. Sodium methylnitraminate (1.0 g, 10 mmol) dissolved in about 10 mL of distilled H_2O was added with stirring, followed by addition of ethylenediamine (0.3 g, 5 mmol). The product was isolated by slow evaporation.

***trans*-Diammine(μ-*N*,*N'*-ethylenedinitraminato)copper(II) Polymer (III).** III was prepared by reaction of an aqueous ammonium hydroxide solution of $Cu(NO_3)_2 \cdot 2.5H_2O$ (5 mmol) and an aqueous solution of the disodium salt of ethylenedinitramine [Na_2(EDNA-2H)] (5 mmol). III was also prepared from the reaction of an aqueous suspension of copper hydroxide (5 mmol) and a warmed aqueous ethanol solution of ethylenedinitramine (10 mmol, protonated ligand). The mixture was stirred for 30 min and filtered, and several milliliters of concentrated ammonium hydroxide was added. The product crystallized within 48 h on standing in a beaker covered with a Kimwipe. Attempts to prepare bis(chelating ligand) complexes of EDNA-2H (e.g., $[Cu(NH_3)_4][Cu(EDNA\text{-}2H)_2]$ and $K_2[Cu(EDNA\text{-}2H)_2]$) were unsuccessful and yielded III instead.

β- and α-Tetraaquo(ethylenedinitraminato)nickel(II) (IV and V). These two polymorphs of the same complex were prepared from $Ni(NO_3)_2 \cdot 6H_2O$ (1.45 g, 5 mmol) or nickel hydroxide (5 mmol) as described above for III. Ammine complexes or a bis(chelating ligand) could not be isolated.

Bis[*mer*-triammine(μ-5-nitraminotetrazolato-*O*,μ-N^1,μ-N^2)nickel(II)] (VI). This complex was prepared by adding an aqueous solution of potassium 5-nitramino-1*H*-tetrazolate (1.68 g, 10 mmol) to nickel hydroxide (5 mmol) partially dissolved in aqueous ammonium hydroxide. After 30 min of stirring and filtration of the cloudy solution over Celite

(2) Liebig, D. M.; Robertson, J. H.; Truter, M. R. *J. Chem. Soc.* **1966**, 879.
(3) Subba Rao, N. S. V.; Ganorkar, M. C.; Mohan Murali, B. K.; Ramaswamy, C. P. *Bull. Acad. Pol. Sci., Ser. Sci. Chim.* **1979**, *27*, 21.
(4) (a) Jones, M. L.; Elrick, D. E.; Herriott, G. E.; Mihlfeith, C. M.; McCarty, K. P. AFRPL-TR-82-079; Air Force Rocket Propulsion Laboratory: Edwards AFB, CA, April 1983. (b) Flanagan, J. E.; Frankel, M. B.; Woolery, D. O. AFRPL-TR-84-044; Air Force Rocket Propulsion Laboratory: Edwards AFB, CA, 1984; (c) Kraeutle, K. J. *CPIA Publ.* **1981**, *2* (*No. 347*), 383.
(5) Willer, R. D., Morton-Thiokol, Inc. personal communication, 1986.
(6) Manser, G. E.; Fletcher, R. W.; Knight, M. R. "High Energy Binders"; Final Report, Pub. No. 85837; Morton-Thiokol: Brigham City, UT, 1985.
(7) Bachman, W. E.; Horton, W. J.; Jenner, E. L.; MacNaughton, W. M.; Maxwell, C. E. *J. Am. Chem. Soc.* **1950**, *72*, 3132.
(8) Henry, R. A.; Lieber, E.; Sherman, E.; Cohen, J. *J. Am. Chem. Soc.* **1951**, *73*, 2327.
(9) Henry, R. A.; Makosky, R. C.; Smith, G. B. L. *J. Am. Chem. Soc.* **1951**, *73*, 474.
(10) Winters, L. J.; Learn, D. B.; Desai, S. C. *J. Org. Chem.* **1965**, *30*, 2471.

Table I. Crystal, Data Collection, and Refinement Parameters

	trans-$[Cu(NH_3)_2(N(NO_2)CH_3)_2]$ (I)	$[Cu(en)(N(NO_2)CH_3)_2]$ (II)	$[Cu(NH_3)_2(EDNA\text{-}2H)]$ (III)	$[Ni(H_2O)_4(EDNA\text{-}2H)]$ (IV)	α-$[Ni(H_2O)_4(EDNA\text{-}2H)]$ (V)	$Ni(NH_3)_3(N_4CNNO_2)]_2$ (VI)	$[Cu(en)_2][Cu_2(en)_2(EDNA\text{-}2H)_3]\cdot 2H_2O$ (VII)
formula	$C_2H_{14}CuN_6O_4$	$C_4H_{14}CuN_6O_4$	$C_2H_{10}CuN_6O_4$	$C_2H_{12}N_4NiO_8$	$C_2H_{12}N_4NiO_8$	$CH_9N_9NiO_2$	$C_{14}H_{48}Cu_3N_{20}O_{14}$
cryst syst	monoclinic	monoclinic	triclinic	monoclinic	monoclinic	monoclinic	triclinic
space group	$P2_1/n$	$P2_1/c$	$P\bar{1}$	$C2/c$	$P2_1/n$	$P2_1/n$	$P\bar{1}$
a, Å	7.3786 (8)	12.282 (3)	5.851 (2)	12.584 (3)	13.508 (2)	7.200 (1)	7.727 (5)
b, Å	6.2543 (8)	9.150 (2)	6.392 (4)	7.867 (2)	11.166 (2)	16.864 (3)	10.248 (6)
c, Å	10.123 (2)	10.563 (3)	6.501 (3)	10.627 (2)	14.133 (2)	7.349 (1)	11.367 (7)
α, deg	90	90	97.24 (4)	90	90	90	90.90 (5)
β, deg	102.00 (1)	113.69 (2)	108.02 (4)	111.18 (2)	114.23 (1)	114.25 (2)	108.26 (5)
γ, deg	90	90	111.46 (4)	90	90	90	96.82 (5)
V, Å^3	457.0 (1)	1087.0 (6)	207.2 (2)	980.9 (5)	1942.3 (5)	813.5 (3)	847.4 (9)
Z	2	4	1	4	8	2	1
D(calcd), g cm^{-3}	1.80	1.67	1.97	1.89	1.90	1.94	2.13
cryst color	purple	purple	purple	blue	blue	dark blue/purple	dark blue/purple
cryst dimens, mm	0.40 × 0.40 × 0.40	0.31 (b) × 0.36 (h)	0.40 × 0.36 × 0.12	0.35 × 0.25 × 0.20	0.40 × 0.40 × 0.28	0.24 × 0.24 × 0.14	0.30 × 0.30 × 0.50
μ (abs coeff), cm^{-1}	24.8	20.20	26.38	19.93	20.11	23.83	19.50
scan speed, deg/min	var, 5–20	var, 5–20	var, 7–20	var, 5–20	var 8–20	var, 5–20	var, 7–20
scan range, deg	$4 \le 2\theta \le 60$	$4 \le 2\theta \le 55$	$4 \le 2\theta \le 60$	$4 \le 2\theta \le 60$	$4 \le 2\theta \le 48$	$4 \le 2\theta \le 55$	$4 \le 2\theta \le 48$
scan method	Wyckoff	$\theta/2\theta$	$\theta/2\theta$	Wyckoff	Wyckoff	$\theta/2\theta$	$\theta/2\theta$
no. of reflcns collcd	1528	2798	1310	1604	3375	2093	2805
no. of indep reflcns	1336	2499	1213	1438	3054	1877	2650
no. of refl with $(F_o) \ge 5\sigma(F_o)$	1048	2093	1207	1156	2105	1295	2383
R(int), %	3.09	1.34	1.82	3.69	10.85	2.14	4.36
std reflcns	3 stds/197 reflcns	3 stds/197 reflcns	3 stds/197 reflcns	3 stds/197 reflcns	3 stds/197 reflcns	3 stds/197 reflcns	3 stds/197 reflcns
data/param ratio	1048/86	2093/137	1207/82	1156/94	2105/335	1295/156	2383/329
GOF	0.950	1.487	1.075	1.098	1.084	0.898	1.469
$R(F)$, %	2.30	3.28	2.16	3.23	4.07	3.89	3.64
$R(wF)$, %	2.72	3.92	2.30	3.28	4.60	4.28	4.10
weighting factor, g	0.001	0.0008	0.0006	0.0004	0.001	0.001	0.001

to remove the unreacted nickel hydroxide gel, the product was obtained by slow evaporation of the filtrate.

Diammine(ethylenedinitroaminato)palladium(II). Palladium chloride (0.9 g, 5 mmol) was suspended in excess concentrated ammonium hydroxide and warmed on a steam bath until dissolution was complete. An aqueous solution of Na_2[EDNA-2H] (5 mmol) was added to the yellow $[Pd(NH_3)_4]Cl_2$ solution. The complex was isolated by slow evaporation. Attempts to prepare a bis(chelating ligand) complex (e.g. $[Pd(NH_3)_4][Pd(EDNA\text{-}2H)_2]$) were unsuccessful.

Bis(ethylenediamine)copper(II) (μ-*N*,*N*′-Ethylenedinitraminato)bis[(ethylenediamine)(*N*,*N*′-ethylenedinitraminato)cuprate(2−)] Dihydrate (VII). A warm aqueous/ethanolic solution of ethylenedinitramine (0.005 mol, 0.75 g) and ethylenediamine (0.005 mol, 0.30 g) was added to an aqueous suspension of copper hydroxide (0.005 mol). After being stirred for 20 min, the purple solution was filtered. The complex was isolated by evaporation or cooling (2 °C) of the filtrate.

Infrared Spectra. Infrared spectra were recorded with a Nicolet 60SX FTIR spectrometer equipped with a MCT-B detector. A total of 32 scans were accumulated at a resolution of 2 cm^{-1}. Spectra were recorded for samples dispersed in a KBr pellet and for neat samples with the sample "burnished" on a single NaCl plate. No differences were observed in the spectra for the two sampling methods.

X-ray Structural Determinations. Crystals of I were grown at 0 °C over a period of several weeks from the preparative mother liquor (water/methanol/ethyl acetate). Crystals of II, III, and VI were obtained by evaporation from aqueous ammonium hydroxide. Crystals of IV, V, and VII were grown by slow evaporation of the aqueous mother liquor.

The crystals were mounted on glass fibers with epoxy cement. Data were collected at ambient temperature (23–25 °C) on a Nicolet R3m/μ diffractometer with graphite-monochromated Mo Kα radiation (λ = 0.71073 Å). The parameters used during data collection and refinement are contained in Table I. Unit cell parameters were derived from the least-squares fit of the angular settings of 25 reflections ($21° \le 2\theta \le 40°$) chosen to include Friedel-related sets to check diffractometer and optical alignment.

On the basis of systematic absences, space groups for I, II, V, and VI were unambiguously assignable. The centrosymmetric space group $P\bar{1}$ and $C2/c$ were chosen for III, IV, and VII, based on systematic absences, the distribution of E values, and the successful solution and refinement of the structures. I, II, III, V, and VII were corrected for absorption by an empirical procedure that employs six refined parameters to define a pseudoellipsoid. Structures I and III were solved intuitively, placing Cu at (0, 0, 0). Structures II, IV, and V were solved by direct methods (SOLV), and VI was solved via heavy-atom methods. All remaining atoms were located from subsequent difference Fourier syntheses. All of the H atoms were located in each complex except for II and V. The methylene hydrogen atoms for II and V were calculated (d(C–H) = 0.96 Å; thermal parameters equal to 1.2 times the isotropic equivalent for the carbon to which it was attached). All non-hydrogen atoms were refined

Table II. Atomic Coordinates (×10^4) and Isotropic Thermal Parameters (Å^2 × 10^3) for I

	x	y	z	U^a
Cu	5000	5000	5000	24 (1)
N(1)	4183 (2)	5928 (4)	6675 (2)	34 (1)
N(2)	7205 (2)	6876 (3)	5432 (2)	31 (1)
N(3)	8554 (2)	5961 (3)	6236 (2)	36 (1)
O(1)	8247 (3)	4088 (3)	6615 (2)	58 (1)
O(2)	10104 (2)	6859 (3)	6628 (2)	56 (1)
C(1)	7548 (4)	9002 (5)	4980 (3)	56 (1)

[a] Equivalent isotropic U defined as one-third of the trace of the orthogonalized U_{ij} tensor.

Table III. Atomic Coordinates (×10^4) and Isotropic Thermal Parameters (Å^2 × 10^3) for II

	x	y	z	U^a
Cu	2447 (1)	5147 (1)	2556 (1)	28 (1)
N(1)	3865 (2)	4691 (3)	2116 (3)	35 (1)
N(2)	1911 (2)	3113 (3)	1870 (2)	34 (1)
N(3)	3159 (2)	7002 (3)	3545 (3)	40 (1)
N(4)	3755 (2)	6702 (3)	4845 (3)	40 (1)
N(5)	890 (2)	5587 (3)	2644 (3)	37 (1)
N(6)	184 (2)	6238 (3)	1532 (2)	36 (1)
O(1)	3793 (2)	5360 (3)	5187 (2)	49 (1)
O(2)	4279 (2)	7673 (3)	5723 (3)	64 (1)
O(3)	601 (2)	6500 (3)	631 (2)	52 (1)
O(4)	−861 (2)	6597 (3)	1334 (2)	52 (1)
C(1)	3630 (3)	3329 (3)	1294 (3)	41 (1)
C(2)	2944 (3)	2297 (3)	1820 (3)	40 (1)
C(3)	3020 (4)	8540 (4)	3169 (4)	60 (2)
C(4)	415 (3)	5313 (4)	3688 (4)	53 (1)

[a] Equivalent isotropic U defined as one-third of the trace of the orthogonalized U_{ij} tensor.

Table IV. Atomic Coordinates (×10⁴) and Isotropic Thermal Parameters (Å² × 10³) for III

	x	y	z	U[a]
Cu	0	10000	0	20 (1)
N(1)	3543 (3)	12736 (2)	1318 (2)	27 (1)
N(2)	899 (2)	8854 (2)	2787 (2)	23 (1)
N(3)	2150 (2)	7620 (2)	2515 (2)	24 (1)
O(1)	2499 (3)	7405 (2)	661 (2)	33 (1)
O(2)	3010 (3)	6678 (3)	3951 (2)	39 (1)
C(1)	569 (3)	9118 (3)	4924 (2)	26 (1)

[a] Equivalent isotropic U defined as one-third of the trace of the orthogonalized $\mathbf{U}_{ij}$ tensor.

Table V. Atomic Coordinates (×10⁴) and Isotropic Thermal Parameters (Å² × 10³) for IV

	x	y	z	U[a]
Ni	960 (1)	2501 (1)	9109 (1)	20 (1)
O(1)	2506 (2)	2460 (2)	9196 (3)	30 (1)
O(2)	728 (2)	1054 (3)	8119 (2)	30 (1)
O(3)	−669 (3)	2495 (3)	8740 (3)	37 (1)
O(4)	703 (2)	3769 (3)	7948 (2)	30 (1)
O(5)	813 (3)	5434 (3)	9300 (3)	36 (1)
O(6)	1789 (3)	5615 (3)	10976 (2)	36 (1)
O(7)	1184 (3)	−360 (3)	9717 (2)	39 (2)
O(8)	1403 (3)	−220 (3)	11331 (2)	39 (1)
N(1)	1351 (3)	3807 (3)	10254 (3)	28 (2)
N(2)	1333 (3)	4944 (3)	10200 (3)	27 (2)
N(3)	1360 (3)	1422 (3)	10417 (3)	25 (1)
N(4)	1317 (3)	286 (3)	10507 (3)	25 (1)
C(1)	1942 (4)	3324 (4)	11307 (3)	35 (2)
C(2)	1505 (4)	2085 (4)	11352 (4)	34 (2)
Ni′	1711 (1)	3559 (1)	5839 (1)	19 (1)
O(1′)	181 (3)	2629 (3)	5827 (3)	33 (1)
O(2′)	2197 (3)	1384 (3)	7058 (2)	29 (1)
O(3′)	3287 (3)	2555 (3)	5955 (3)	33 (1)
O(4′)	2118 (3)	3951 (3)	6891 (2)	30 (1)
O(5′)	1255 (2)	5425 (3)	5227 (2)	32 (1)
O(6′)	1170 (3)	5316 (3)	3639 (2)	38 (1)
O(7′)	1572 (3)	−366 (2)	5635 (2)	36 (1)
O(8′)	714 (3)	−538 (3)	3945 (2)	35 (1)
N(1′)	1205 (3)	3640 (3)	4527 (3)	24 (1)
N(2′)	1212 (3)	4784 (3)	4445 (3)	26 (1)
N(3′)	1221 (3)	1262 (3)	4672 (3)	24 (1)
N(4′)	1157 (3)	127 (3)	4735 (3)	23 (1)
C(1′)	1127 (4)	2999 (4)	3597 (3)	33 (2)
C(2′)	698 (4)	1736 (4)	3615 (3)	34 (2)

[a] Equivalent isotropic U defined as one-third of the trace of the orthogonalized $\mathbf{U}_{ij}$ tensor.

Table VI. Atomic Coordinates (×10⁴) and Isotropic Thermal Parameters (Å² × 10³) for V

	x	y	z	U[a]
Ni	5000	2033.7 (5)	2500	27.8 (1)
O(1)	3539 (1)	1939 (3)	2972 (2)	39 (1)
O(2)	4325 (2)	145 (3)	1075 (2)	47 (1)
O(3)	3477 (2)	2745 (3)	−727 (2)	56 (1)
O(4)	3053 (1)	5419 (3)	−545 (2)	56 (1)
N(1)	4373 (2)	4094 (3)	1181 (2)	34 (1)
N(2)	3633 (2)	4094 (3)	−28 (2)	39 (1)
C(1)	4472 (3)	5724 (3)	1886 (3)	48 (1)

[a] Equivalent isotropic U defined as one-third of the trace of the orthogonalized $\mathbf{U}_{ij}$ tensor.

anisotropically for the seven structures. Structures I and III were corrected for secondary extinction effects.

The atomic coordinates for I–VII appear in Tables II–VIII, respectively. Selected bond distances and angles appear in the text. Additional crystallographic data and packing diagrams are available as supplementary material.

Structural Studies

Unidentate N-Coordination with Weak M···O Interaction (1). Two Cu(II) complexes of $CH_3NNO_2^-$, *trans*-$Cu(NH_3)_2[N(NO_2)CH_3]_2$ (I) and $Cu(en)[N(NO_2)CH_3]_2$ (II) were synthesized and structurally characterized. Tables IX and X give selected bond distances and angles for these two complexes. Figures 1 and 2 illustrate the structural features. The structural data for polymeric *trans*-$Cu(NH_3)_2$(EDNA-2H) (III) are also directly comparable in this mode of coordination. Table XI and Figure 3 summarize the structural details for a repeating fragment of this compound.

The heavy atoms of the methylnitraminato ligand and the Cu atom approximately form a plane. The N–N bond distances of

Table VII. Atomic Coordinates (×10⁴) and Isotropic Thermal Parameters (Å² × 10³) for VI

	x	y	z	U[a]
Ni	5957 (1)	3908 (1)	6066 (1)	22 (1)
Ni(1)	3018 (5)	4345 (2)	4408 (5)	26 (1)
N(2)	1480 (6)	3849 (2)	3810 (7)	33 (1)
N(3)	−223 (6)	4258 (2)	2748 (7)	36 (2)
N(4)	2383 (5)	5085 (2)	3802 (5)	23 (1)
N(5)	−1171 (6)	5553 (2)	1780 (7)	35 (2)
N(6)	−724 (6)	6274 (2)	1613 (6)	30 (1)
N(7)	6149 (6)	3491 (3)	3476 (6)	29 (2)
N(8)	4792 (7)	2800 (3)	6393 (8)	36 (2)
N(9)	5769 (8)	4261 (4)	8723 (7)	34 (2)
C	356 (6)	5005 (3)	2764 (7)	26 (2)
O(1)	−2192 (5)	6735 (2)	731 (6)	44 (1)
O(2)	1053 (5)	6570 (2)	2257 (6)	39 (1)

[a] Equivalent isotropic U defined as one-third of the trace of the orthogonalized $\mathbf{U}_{ij}$ tensor.

Table VIII. Atomic Coordinates (×10⁴) and Isotropic Thermal Parameters (Å² × 10³) for VII

	x	y	z	U[a]
Cu(1)	5000	0	10000	23 (1)
Cu(2)	7672 (1)	3205 (1)	7055 (1)	21 (1)
N(1)	7290 (4)	5265 (3)	6653 (2)	26 (1)
N(2)	5453 (4)	3445 (3)	7570 (2)	24 (1)
N(3)	8185 (4)	6129 (3)	6168 (2)	26 (1)
N(4)	4619 (3)	2551 (3)	8048 (2)	26 (1)
N(5)	9733 (4)	2945 (3)	6381 (2)	26 (1)
N(6)	6182 (4)	1868 (3)	5661 (2)	28 (1)
N(7)	9494 (3)	3588 (2)	8811 (2)	21 (1)
N(8)	10123 (3)	2566 (3)	9349 (2)	24 (1)
O(1)	7573 (3)	7202 (2)	5790 (2)	39 (1)
O(2)	9710 (3)	5901 (2)	6083 (2)	42 (1)
O(3)	5058 (4)	1401 (2)	8063 (2)	44 (1)
O(4)	3382 (4)	2804 (3)	8502 (2)	45 (1)
O(5)	11313 (3)	2613 (2)	10402 (2)	35 (1)
O(6)	9454 (3)	1451 (2)	8757 (2)	33 (1)
O_w	6851 (4)	9348 (3)	7083 (2)	44 (1)
C(1)	5560 (4)	5616 (3)	6731 (3)	32 (1)
C(2)	4935 (5)	4759 (3)	7627 (3)	36 (1)
C(3)	9255 (5)	1689 (3)	5632 (3)	31 (1)
C(4)	7274 (5)	1603 (4)	4849 (3)	38 (1)
C(5)	10378 (4)	4847 (3)	9470 (3)	26 (1)
N(9)	7731 (4)	360 (3)	10695 (2)	28 (1)
N(10)	5007 (4)	1611 (3)	11033 (3)	27 (1)
C(6)	8212 (4)	1341 (4)	11748 (3)	34 (1)
C(7)	6876 (5)	2328 (3)	11416 (3)	31 (1)

[a] Equivalent isotropic U defined as one-third of the trace of the orthogonalized $\mathbf{U}_{ij}$ tensor.

Table IX. Bond Distances and Angles for $Cu(NH_3)_2[N(NO_2)CH_3]_2$ (I)

Bond Distances (Å)			
Cu–N(1)	2.000 (2)	Cu–N(2)	1.980 (1)
Cu–N(1A)	2.000 (2)	Cu–N(2A)	1.980 (1)
N(2)–N(3)	1.282 (2)	N(2)–C(1)	1.446 (4)
N(3)–O(1)	1.268 (3)	N(3)–O(2)	1.262 (4)
Bond Angles (deg)			
N(1)–Cu–N(2)	91.1 (1)	N(1)–Cu–N(1A)	180.0 (1)
N(2)–Cu–N(1A)	88.9 (1)	N(1)–Cu–N(2A)	88.9 (1)
N(2)–Cu–N(2A)	180.0 (1)	N(1A)–Cu–N(2A)	91.1 (1)
Cu–N(2)–N(3)	111.7 (1)	Cu–N(2)–C(1)	131.7 (1)
N(3)–N(2)–C(1)	116.6 (2)	N(2)–N(3)–O(1)	116.2 (2)
N(2)–N(3)–O(2)	122.3 (2)	O(1)–N(3)–O(2)	121.6 (2)

Table X. Bond Distances and Angles for $Cu(en)[N(NO_2)CH_3]_2$ (II)

	Bond Distances (Å)		
Cu–N(1)	2.019 (3)	Cu–N(2)	2.009 (2)
Cu–N(3)	2.001 (2)	Cu–N(5)	1.992 (3)
N(3)–N(4)	1.300 (3)	N(3)–C(3)	1.453 (4)
N(4)–O(1)	1.275 (4)	N(4)–O(2)	1.259 (3)
N(5)–N(6)	1.291 (3)	N(5)–C(4)	1.462 (6)
N(6)–O(3)	1.272 (4)	N(6)–O(4)	1.258 (3)
	Bond Angles (deg)		
N(1)–Cu–N(2)	85.0 (1)	N(1)–Cu–N(3)	93.4 (1)
N(2)–Cu–N(3)	170.1 (1)	N(1)–Cu–N(5)	170.3 (1)
N(2)–Cu–N(5)	91.3 (1)	N(3)–Cu–N(5)	91.8 (1)
Cu–N(3)–N(4)	108.4 (2)	Cu–N(3)–C(3)	134.4 (2)
N(4)–N(3)–C(3)	116.6 (3)	N(3)–N(4)–O(1)	116.3 (2)
N(3)–N(4)–O(2)	122.2 (3)	O(1)–N(4)–O(2)	121.4 (2)
Cu–N(5)–N(6)	110.9 (2)	Cu–N(5)–C(4)	133.0 (2)
N(6)–N(5)–C(4)	116.1 (3)	N(5)–N(6)–O(3)	116.3 (3)
N(5)–N(6)–O(4)	122.6 (3)	O(3)–N(6)–O(4)	121.1 (2)

Table XI. Bond Distances and Angles for Poly-$Cu(NH_3)_2$(EDNA-2H) (III)

	Bond Distances (Å)		
Cu–N(1)	1.990 (1)	Cu–N(2)	2.030 (1)
Cu–N(1A)	1.990 (1)	Cu–N(2A)	2.030 (1)
N(2)–N(3)	1.287 (2)		
N(3)–O(1)	1.283 (2)	N(3)–O(2)	1.249 (2)
	Bond Angles (deg)		
N(1)–Cu–N(2)	90.6 (1)	N(1)–Cu–N(1A)	180.0 (1)
N(2)–Cu–N(1A)	89.4 (1)	N(1)–Cu–N(2A)	89.4 (1)
N(2)–Cu–N(2A)	180.0 (1)	N(1A)–Cu–N(2A)	90.6 (1)
Cu–N(2)–N(3)	107.2 (1)	Cu–N(2)–C(1)	137.4 (1)
	115.4 (1)	N(2)–N(3)–O(1)	116.2 (1)
N(2)–N(3)–O(2)	123.2 (2)	O(1)–N(3)–O(2)	120.6 (2)
	107.7 (2)		

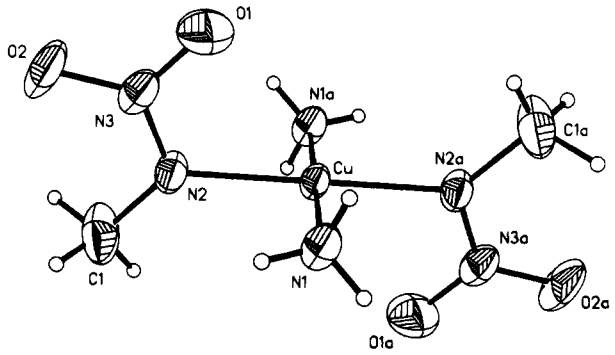


Figure 1. Molecular structure of *trans*-$Cu(NH_3)_2[N(NO_2)CH_3]_2$ (I), showing 50% probability ellipsoids. A weak axial interaction exists between Cu(II) and O(1) and O(1a).

1.282–1.300 (3) Å in the three complexes are substantially shorter than the N–N distances of 1.36–1.38 Å found with secondary organic nitramines.[11-16] The N–N bond lengths more closely resemble those in the neutral primary nitramine, EDNA[17] (1.30 Å), and Na_2(EDNA-2H)[18] (1.28 Å), which is good evidence that a significant amount of negative charge is retained on the nitramine ligand even after it coordinates to the metal atom and that the N–N bond possesses substantial double-bond character. In

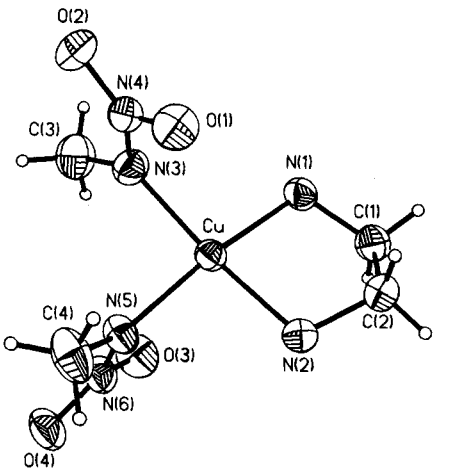


Figure 2. Molecular structure of $Cu(en)[N(NO_2)CH_3]_2$ (II), showing 50% probability ellipsoids. The H atoms on the ethylenediamine N atoms are not shown because they were not located experimentally. A weak axial interaction exists between Cu(II) and O(1) and O(3).

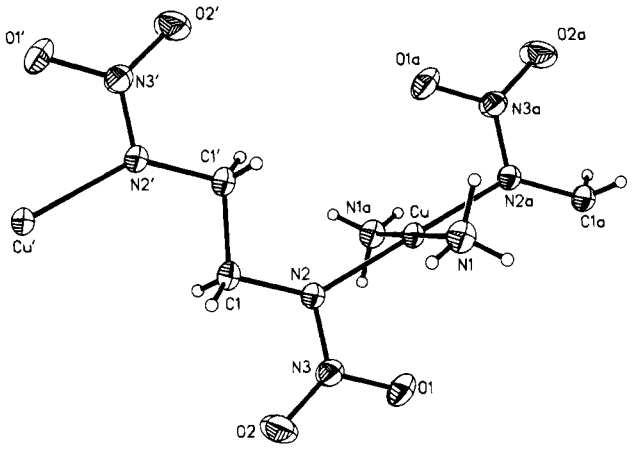


Figure 3. Fragment of poly-$[Cu(NH_3)_2$(EDNA-2H)] (III), showing the 50% probability ellipsoids. A weak axial interaction exists between Cu(II) and O(1) and O(1a).

part compensating for the large N–N double-bond character is the fact that the N–O bond distances are significantly longer (1.249–1.275 (3) Å) in these metal complexes compared to those in secondary nitramines (1.21–1.24 Å).[11-16] Even for a primary nitramine the N–O bond distance is less than 1.24 Å.[17] However, the N–O bonds lengthen to about 1.29 Å in Na_2(EDNA-2H).[18] Hence, the distribution of π-electron density within the nitramine groups can shift between the N–N and N–O bonds. The π-electron density is higher in the N–N bond and lower in the N–O bond in metal–nitraminato complexes and nitramine anions, whereas the reverse is true in the organic secondary nitramines.

The steric requirements of the nitraminato ligand favor an anti arrangement of the nitro groups given that the atom positions about the nitrogen atom must remain essentially planar. This places an oxygen atom in the region above and below the CuN_4 plane. There is circumstantial evidence that these oxygen atoms are weakly coordinated to the Cu atom. The Cu···O distance, O···Cu–N angle and Cu–N–N angle for each compound would be expected to follow a consistent pattern if Cu···O interaction occurs. Table XII compiles these data. As the Cu···O distance becomes shorter, the improved overlap leads to an increase in the O···Cu–N angle. In turn, to accommodate this larger angle, the internal Cu–N–N angle in the nitramine ligand should become progressively smaller. These trends are found with the three compounds. The Cu···O separation of 2.58–2.67 Å is much longer than a full Cu–O covalent bond (ca. 1.96 Å).[19] The observed

(11) Oyumi, Y.; Brill, T. B.; Rheingold, A. L. *J. Phys. Chem.* **1985**, *89*, 4824.
(12) Oyumi, Y.; Brill, T. B.; Rheingold, A. L. *J. Phys. Chem.* **1986**, *90*, 2526.
(13) Oyumi, Y.; Rheingold, A. L.; Brill, T. B. *J. Phys. Chem.* **1986**, *90*, 4686.
(14) Oyumi, Y.; Rheingold, A. L.; Brill, T. B. *Propellants Explos. Pyrotech.* **1987**, *12*, 1.
(15) Oyumi, Y.; Brill, T. B.; Rheingold, A. L. *Thermochim. Acta* **1987**, *114*, 209.
(16) Lowe-Ma, C. K.; Willer, R. L. NWC TP-6681; Naval Weapons Center: China Lake, CA, Oct. 1987.
(17) Turley, J. A. *Acta Crystallogr., Sect. B: Struct. Crystallogr. Cryst. Chem.* **1968**, *B24*, 942.
(18) Allentoff, N.; Wright, G. F. *Acta Crystallogr.* **1953**, *6*, 1.
(19) Duffin, B. *Acta Crystallogr., Sect. B: Struct. Crystallogr. Cryst. Chem.* **1968**, *B24*, 396.

Table XII. Data Trends Supporting a Weak Axial Cu···O Association in Copper–Nitraminato and Other Complexes

compd	Cu···O, Å	O···Cu–N, deg	Cu–N(amine)–N(nitro), deg	"off the z axis" angle, deg
poly-$Cu(NH_3)_2$(EDNA-2H)	2.58	55.0	107.2	35
$Cu(en)[N(NO_2)CH_3]_2$	2.63[a]	54.1	109.6[a]	36[a]
$Cu(NH_3)_2[N(NO_2)CH_3]_2$	2.67	53.1	111.7	37
$Cu(bpy)(ONO)_2$[20]	2.48–2.51	54.2, 55.0		32
$Cu[o\text{-}Ph(CO_2)_2]\cdot 2H_2O$[21]	2.68	54.4		36
$Cu(2\text{-pic})_2(ClCH_2CO_2)_2$[22,b]	2.71	53.9		36
$Cu(CH_3CO_2)_2(NH_3)_2$[23]	2.77	52.8		40

[a] Average value. [b] 2-pic = 2-picoline.

Table XIII. Selected Bond Distances (Å)[2] for Diaquo(tetramethylenedinitraminato)nickel(II)

Ni–O(1)	1.991 (9)	N(2)–O(2)	1.362 (12)
Ni–O(2)	2.156 (9)	N(2)–O(3)	1.325 (13)
Ni–N(1)	2.234 (10)	N(1)–N(2)	1.240 (14)

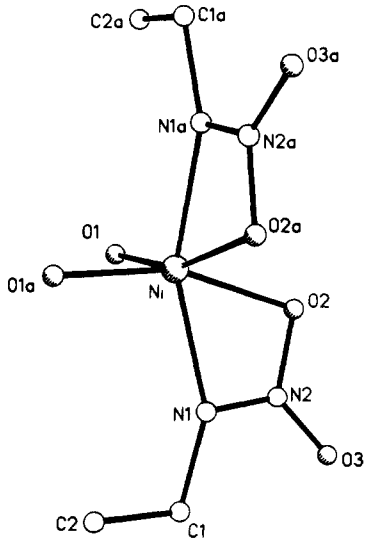


Figure 4. Structure of a fragment of poly-$\{Ni(H_2O)_2[N(NO_2)(CH_2)_4N(NO_2)]\}$ illustrating the coordination sphere of the Ni(II) atom (modified from ref 2). H atoms are not shown.

Cu···O distances and the related angles are similar to those of other Cu(II) complexes with presumed axial "semicoordination"[20-23] which are also shown in Table XII. The axial coordination of such complexes has been described as out-of-plane or off-the-z-axis bonding. Hathaway has discussed the relevance and experimental evidence for this (4 + 0 + 2*) coordination in Cu(II) complexes.[24,25]

The crystal packing of I and II is controlled mostly by N–H···O hydrogen bonding as evidenced by the heavy-atom distances.

Bidentate Covalent N,O-Coordination (2). The crystal structure of poly$\{Ni[N(NO_2)(CH_2)_4N(NO_2)](H_2O)_2\}_x$ found by Liebig et al.[2] to contain a four-membered ring in which the N–NO_2 group forms a four-membered chelate ring with the Ni atom. This result is summarized here because it is the only structurally characterized example of a complex in which both the oxygen atom and amine nitrogen atom are covalently bonded to the same metal atom. Figure 4 shows the structure of the repeating unit. Table XIII summarizes some of the pertinent bond distances for comparison with the other values in this paper.

Unidentate O-Coordination (3). 5-Nitramintetrazolate forms a metal complex in which an oxygen atom of the nitramine group coordinates to the metal atom without participation from the amine nitrogen atom. Figure 5 shows the structure of $[Ni(NH_3)_3(O_2NNCN_4)]_2$ (VI), and Table XIV gives selected bond distances and angles. The dimer is assembled through *mer* coordination of NH_3 to two Ni atoms with two nitrogen atoms for each tetrazole ring producing the bridging sites. The six-membered $NiN_2Ni'N_2'$ ring is essentially planar. The nitrogen atom of the tetrazolato ring that coordinates to the nickel atom is in a position such that it and the oxygen atom of the nitraminato group are able form a second, essentially planar, six-membered chelate ring with Ni(II). The amine nitrogen atom of the nitramine group is deprotonated and is forced away from the nickel atom. It is not inolved in any close interaction with neighboring molecules.

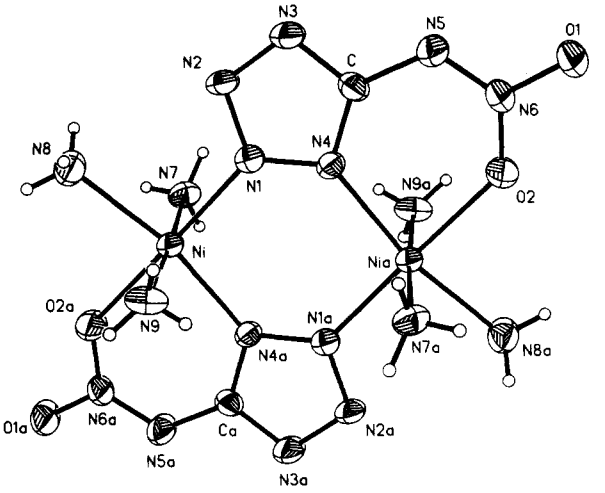


Figure 5. Molecular structure of the $[Ni(NH_3)_3(O_2NNCN_4)]_2$ dimer (VI). The 50% probability ellipsoids are shown.

Table XIV. Bond Distances and Angles for $[Ni(NH_3)_3(O_2NNCN_4)]_2$ (VI)

Bond Distances (Å)			
Ni–N(1)	2.095 (3)	Ni–N(7)	2.086 (5)
Ni–N(8)	2.103 (5)	Ni–N(9)	2.099 (6)
Ni–N(4A)	2.055 (4)	Ni–O(2A)	2.150 (3)
N(1)–N(2)	1.312 (5)	N(1)–N(4)	1.340 (5)
N(2)–N(3)	1.343 (5)	N(3)–C	1.324 (6)
N(4)–C	1.347 (5)		
N(5)–N(6)	1.276 (6)	N(5)–C	1.391 (6)
N(6)–O(1)	1.257 (5)	N(6)–O(2)	1.270 (5)
Bond Angles (deg)			
N(1)–Ni–N(7)	91.0 (2)	N(1)–Ni–N(8)	91.4 (2)
N(7)–Ni–N(8)	89.1 (2)	N(1)–Ni–N(9)	90.3 (2)
N(1)–Ni–N(4A)	99.5 (1)	N(8)Ni–N(9)	88.0 (2)
N(4A)–Ni–O(2A)	81.8 (1)	N(6)–N(5)–C	120.5 (4)
N(5)–N(6)–O(1)	116.6 (4)	N(5)–N(6)–O(2)	126.4 (4)
O(1)–N(6)–O(2)	117.1 (4)		

The N–N bond distance of the nitramine group (1.276 (6) Å) is close to that of a double bond (1.24 Å) while the N–O bonds are slightly longer (1.257 (5), 1.270 (5) Å) than those of organic nitramines (1.21–1.24 Å).[11-16] As expected, the N–O bond distance of the coordinated oxygen atom is longer than the N–O bond of the unassociated oxygen atom. The distance separating the Ni atoms in the dimer (4.017 (4) Å) suggests that little through-space interaction between nickel atoms is possible.

(20) Stephens, F. S. *J. Chem. Soc. A* **1969**, 2081.
(21) Cingi, M. B.; Guastini, C.; Musatti, A.; Nardelli, M. *Acta Crystallogr., Sect. B: Struct. Crystallogr. Cryst. Chem.* **1969**, *B25*, 1833.
(22) Stephens, F. S.; Davey, G. *J. Chem. Soc. A* **1971**, 1917.
(23) Simonov, Y. A.; Ablov, A. V.; Malinovski, T. I. *Kristallografiya* **1963**, *8*, 205.
(24) Hathaway, B. J. *Struct. Bonding (Berlin)* **1973**, *14*, 49.
(25) Hathaway, B. J. *Struct. Bonding (Berlin)* **1984**, *57*, 107.

Table XV. Bond Distances and Angles for β-$Ni(H_2O)_4$(EDNA-2H) (IV)

	Bond Distances (Å)		
Ni–O(1)	2.075 (2)	Ni–O(2)	2.072 (2)
Ni–N(1)	2.102 (2)	Ni–O(1A)	2.074 (2)
Ni–O(2A)	2.072 (2)	Ni–N(1A)	2.102 (2)
O(3)–N(2)	1.269 (3)	O(4)–N(2)	1.277 (3)
N(1)–N(2)	1.285 (2)		
	Bond Angles (deg)		
O(1)–Ni–O(2)	89.2 (1)	O(1)–Ni–N(1)	92.1 (1)
O(2)–Ni–N(1)	96.3 (1)		
O(2)–Ni–N(1)	87.8 (1)	N(1)–Ni–O(1A)	91.1 (1)
O(1)–Ni–O(2A)	87.8 (1)	O(2)–Ni–O(2A)	88.3 (1)
		O(1A)–Ni–O(2A)	89.2 (1)
O(1)–Ni–N(1A)	91.1 (1)	O(2)–Ni–N(1A)	175.3 (1)
N(1)–Ni–N(1A)	79.0 (1)	O(1A)–Ni–N(1A)	92.1 (1)
O(2A)–Ni–N(1A)	96.3 (1)	Ni–N(1)–N(2)	128.9 (2)
O(3)–N(2)–O(4)	119.1 (2)	O(3)–N(2)–N(1)	119.2 (2)
O(4)–N(2)–N(1)	121.6 (2)		

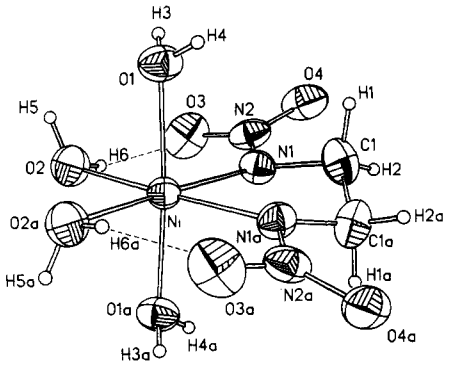


Figure 6. Molecular structure of β-$[Ni(H_2O)_4$(EDNA-2H)] (IV), showing 50% probability ellipsoids and the intramolecular hydrogen bonding.

In the crystal packing of this complex, the molecules are stacked in columns based on what appears to be the geometric test fit. The shortest intermolecular heavy-atom contact is O(1)···N(7) of 3.052 (5) Å, suggesting that weak N–H···O hydrogen bonding may exist between these sites.

An attempt was made to obtain an entirely O-bonded nitramine without assistance from other coordination sites in the molecule by reacting *tert*-butylnitramine with copper hydroxide. Despite many attempts, crystals suitable for X-ray diffraction were not obtained. Without structural proof it is uncertain how this nitramine coordinates to the copper ion.

Bidentate N,N′-Coordination (4). The trigonal-planar arrangement of σ-bonding electron pairs about the amine nitrogen atom does not restrict the EDNA-2H dianion from forming a chelate with Ni(II). Two polymorphs of $Ni(H_2O)_4$(EDNA-2H) were isolated, structurally characterized, and found to possess bidentate EDNA-2H. Selected intramolecular bond distances and angles for the β-morph are given in Table XV. These data for the α-morph are given in the supplementary material. The molecular structure of the complex is very similar in the two crystal lattices so that Figure 6 suffices to illustrate the molecule. A plane of symmetry relates the halves of the molecule in β-$[Ni(H_2O)_4$(EDNA-2H)] (IV) so that the asymmetric unit contains half of a molecule. The asymmetric unit of α-$[Ni(H_2O)_4$(EDNA-2H)] (V) contains two molecules.

The N–N and N–O bond distances of IV and V are similar to those for the unidentate mode of coordination of the dinitramines discussed above. The NiN_2O_2C atoms do not lie entirely in a plane, but the deviations follow no systematic pattern. Intramolecular hydrogen bonding between the equatorial water molecules and two of the oxygen atoms of EDNA-2H occurs in both morphs and possibly contributes to the secondary geometric features of these molecules.

In IV and V the total number of intra- and intermolecular hydrogen bonds is the same. The principal differences between

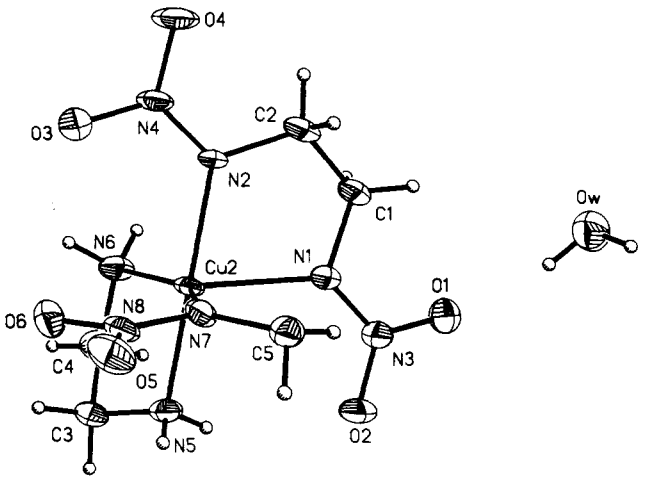


Figure 7. Projection of half of the anion of $[Cu(en)_2][Cu_2(en)_2$(EDNA-2H)$_3]\cdot 2H_2O$ (VII). Two of the EDNA-2H ligands chelate the Cu(II) centers while the third bridges the two Cu(II) centers through C(5). The water of crystallization is hydrogen-bonded O(1) and is involved in cohesive lattice hydrogen bonding.

the α- and β-polymorphs of $Ni(H_2O)_4$(EDNA-2H) occur in the three-dimensional network of these intermolecular hydrogen bonds. The two crystallographically independent molecules of the α-morph are paired face-to-face and linked with hydrogen bonds involving the equatorial water molecules. These pairs are then hydrogen bonded to neighboring pairs via the axial and equatorial water molecules and the oxygen atoms of the nitro groups. The O–H···O hydrogen-bonding network in the β-morph does not produce discernible pairs, but, nevertheless, involves a three-dimensional network as found in the α-morph. In IV each "inside" nitro oxygen atom (O(3), O(3a)) is involved in one intermolecular hydrogen bond, while each "outside" nitro oxygen atom (O(4), O(4a)) is involved in two intermolecular hydrogen bonds.

A palladium complex of the stoichiometry $Pd(NH_3)_2$(EDNA-2H) was synthesized. Although disorder existed that precluded an accurate determination of the bond distances and angles,[26] it is clear from the structure that the EDNA-2H ligand forms a bidentate chelate toward Pd(II) via the nitrogen atoms. In addition, the structure of a six-membered chelate ring involving the propylenedinitraminato dianion and Ni(II) has been reported previously.[1] The bond distances and angles resemble those of the EDNA-2H complexes described here.

Crystalline Polymeric Structures (5). In addition to chelate formation, the terminal dinitraminato ligands bridge adjacent metal ions forming crystalline chains with Cu(II) and Ni(II). Two examples of this mode of coordination are discussed above in connection with the donor sites. The chains of poly-$[Cu(NH_3)_2$(EDNA-2H)] (III) and poly-$\{Ni(H_2O)_2[N(NO_2)(CH_2)_4N(NO_2)]\}$[2] pack similarly in parallel fashion.

Ethylenedinitraminato(2−): Bridging vs N,N′-Chelation. Many factors contribute to the bonding mode of a ligand. In the absence of an overriding factor, a complex containing a chelate ring is expected when a ligand capable of forming a five-membered ring with the metal is employed.[27] Consistent with this, EDNA-2H forms chelate complexes with Ni(II), (IV, V) and Pd(II).[26] However, with Cu(II), EDNA-2H functions as a bridging or

(26) Crystal data for $Pd(NH_3)_2[N(NO_2)(CH_2)_2N(NO_2)]$, orthorhombic, *Pbcm* $a = 3.897$ (2) Å, $b = 16.474$ (9) Å, $c = 12.789$ (6) Å, $V = 820.9$ (7) Å^3, $Z = 4$, $R = 8.25\%$, $R_w = 9.29\%$. The compound contains a chelated EDNA-2H ligand with an approximately 2-fold disorder in the position of the complex in the lattice.

(27) Ethylenediamine and N,N′-substituted ethylenediamine derivatives rarely function as bridging ligands. Four complexes involving Cu(I),[a] Pt(IV),[b] W(III),[c] and Ru(III)[d] have been structurally characterized: (a) Floriani, C.; Pasquali, M.; Gaetani-Manfredotti, A. *Inorg. Chem.* **1980**, *19*, 1191. (b) Robson, A.; Truter, M. R. *J. Chem. Soc.* **1965**, 630. (c) Chisholm, M. H.; Chetcuti, M. J.; Huffman, J. C.; Leonelli, J. *J. Am. Chem. Soc.* **1983**, *105*, 292. (d) Griffith, W. P.; McManus, N. T.; Skapski, A. C. *J. Chem. Soc., Chem. Commun.* **1984**, 484.

Table XVI. Selected Bond Distances (Å) for the Anion of $[Cu(en)_2][Cu_2(en)_2(EDNA\text{-}2H)_3]\cdot 2H_2O$ (VII)

Cu(2)–N(1)	2.201 (3)	N(8)–O(5)	1.256 (3)
Cu(2)–N(5)	2.013 (3)	N(8)–O(6)	1.283 (3)
Cu(2)–N(7)	2.051 (2)	Cu(2)–N(2)	2.017 (3)
N(3)–O(1)	1.276 (3)	Cu(2)–N(6)	2.031 (2)
N(3)–O(2)	1.261 (4)	N(1)–N(3)	1.294 (4)
N(4)–O(3)	1.263 (4)	N(2)–N(4)	1.283 (4)
N(4)–O(4)	1.269 (4)	N(7)–N(8)	1.289 (4)

Table XVII. Selected Angles (deg) for $[Cu(en)_2][Cu_2(en)_2(EDNA\text{-}2H)_3]\cdot 2H_2O$ (VII)

N(1)–Cu(2)–N(2)	77.1 (1)	N(1)–Cu(2)–N(5)	101.9 (1)
N(2)–Cu(2)–N(5)	174.8 (1)	N(1)–Cu(2)–N(6)	114.5 (1)
N(2)–Cu(2)–N(6)	92.2 (1)	N(5)–Cu(2)–N(6)	83.6 (1)
N(1)–Cu(2)–N(7)	96.5 (1)	N(2)–Cu(2)–N(7)	94.2 (1)
N(5)–Cu(2)–N(7)	91.0 (1)	N(6)–Cu(2)–N(7)	148.9 (1)
Cu(2)–N(1)–N(3)	130.4 (2)		
		Cu(2)–N(2)–N(4)	124.0 (2)
		N(4)–N(2)–C(2)	115.7 (3)
N(1)–N(3)–O(1)	121.8 (3)	N(1)–N(3)–O(2)	118.5 (3)
O(1)–N(3)–O(2)	119.7 (3)	N(2)–N(4)–O(3)	118.4 (3)
N(2)–N(4)–O(4)	121.4 (3)	O(3)–N(4)–O(4)	120.2 (3)
Cu(2)–N(7)–N(8)	114.6 (2)	Cu(2)–N(7)–C(5)	129.7 (2)
		N(7)–N(8)–O(5)	123.8 (2)
N(7)–N(8)–O(6)	116.5 (2)	O(5)–N(8)–O(6)	119.7 (2)

chelating ligand. In the previously discussed complex $[Cu(NH_3)_2(EDNA\text{-}2H)]_2$ (III), EDNA-2H functions solely as a bridging ligand. In $[Cu(en)_2][Cu_2(en)_2(EDNA\text{-}2H)_3]\cdot 2H_2O$ (VII), EDNA-2H functions as both a chelating and bridging ligand. The anion (shown in Figure 7) is dimeric, with the copper ions linked by a single bridging EDNA-2H ligand. In addition each copper ion is coordinated to a chelating EDNA-2H ligand. The bite angle is 77.1 (1)°. The coordination is unsymmetric with a Cu(1)–N(2) bond distance of 2.017 (3) Å and a Cu(1)–N(1) bond distance of 2.201 (3) Å. The copper atoms occupy a distorted trigonal-bipyramidal environment with the nitro system oxygen atoms of the EDNA-2H ligands at nonbonded distances. The cation structure is depicted in Figure 8. The cation displays classical Cu(II) 4 + 2 coordination. The elongated tetragonal octahedral environment of Cu(2) is completed by axial interaction of the O(3) oxygen atoms from adjacent dimeric anions. The bond lengths and bond angles are summarized in Tables XVI and XVII.

The tendency for EDNA-2H to function as a bridging ligand with Cu(II) is best explained by the effects of chelate stabilization. Bidentate ligands that impose a higher steric requirement for chelation are expected to exhibit lower chelate stabilization energies for Cu(II) because of the prolate shape of the ion.[24] Atkinson and Bauman[28] compared the free energies of chelation for the en–NH_3 and bipyridine–pyridine (bpy–py) systems with Ni(II) and Cu(II). They demonstrated that in going from Ni(II) to Cu(II), the chelate stabilization energy increases for the en–NH_3 system but decreases for the bpy–py system.

The bite angle for ethylenediamine in Ni(II) and Cu(II) complexes is typically 85–86° (normalized bite[29] $\simeq$ 1.35 Å). For bpy the bite angle averages 79–81° (normalized bite $\simeq$ 1.28 Å). The data for structures IV and V indicate that EDNA-2H imposes a bite angle of 79–80°, with a normalized bite of 1.25–1.28 Å. Note unexpectedly the steric requirement imposed by a chelating EDNA-2H ligand is similar to that of bpy (both ligands have trigonal-planar donor atom geometries). Thus, the chelate stabilization energy for the Cu(II)–(EDNA-2H) system should not be as favorable as for the Ni(II)–(EDNA-2H) system. For Pd(II), chelating EDNA-2H coordination is expected since the larger 4d orbitals can easily accommodate the bite requirements of the ligand.

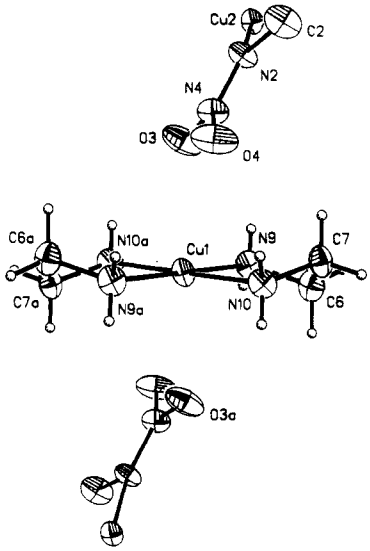


Figure 8. Projection of the cation of $[Cu(en)_2][Cu_2(en)_2(EDNA\text{-}2H)_3]\cdot 2H_2O$ (VII), showing fragments of two of the neighboring anions that engage in weak axial Cu(II)···O interactions.

Table XVIII. Pattern of the Asymmetric NO_2 Stretching Frequency with Respect to the Mode of Coordination of the Nitramine Ligand

compd	coordination (mode)	$\nu_{as}(NO_2)$, cm^{-1}
EDNA		1595[a]
Na_2[EDNA-2H]	salt, free ligand	1462
$[Cu(NH_3)_2(EDNA\text{-}2H)]_x$	strong N, weak O (**1**)	1422
$[Cu(en)_2][Cu_2(en)_2(EDNA\text{-}2H)_3]\cdot 2H_2O$	Strong N (**4**, **5**)	1380
$[Pd(NH_3)_2(EDNA\text{-}2H)]$	strong N (**4**)	1398
$[Ni(H_2O)_4(EDNA\text{-}2H)]$	strong N (**4**)	1409[b]
$K[\overline{NNNN(H)CNNO_2}]$	salt, free ligand	1440
$[Ni(NH_3)_3(\overline{NNNNCNNO_2})]_2$	strong O (**3**)	1482

[a] $\nu_{as}(NO_2)$ strongly coupled with δ(N–H). [b] Broadened by extensive hydrogen bonding.

Infrared Spectra. It is possible that the infrared absorptions that are largely localized on the nitramine group might reflect some of the bond-distance trends. We have shown previously that a trend exists between the N–N bond distance and $\nu_{as}(NO_2)$ for secondary nitramines.[14] This relationship is not observed for primary nitramines, their salts, or the present metal complexes. It is likely that differences in the coupling defeat the correlation over a broad range of compounds. $\nu_{as}(NO_2)$ in secondary nitramines is coupled with the N–N stretching mode. In primary nitramines $\nu_{as}(NO_2)$ is also coupled with the N–H bending mode. In most of our metal–nitramine complexes, coupling between the $-NO_2$ stretching modes and the deformation modes of coordinated ammonia is probable and is similar to that observed in amminenitrometal complexes.[31]

Despite these considerations there is a qualitative trend between the $\nu_{as}(NO_2)$ and the coordination mode of the nitramine ligand (see Table XVIII). Strong nitro oxygen coordination (mode **3**) raises the $\nu_{as}(NO_2)$ compared to that in the free ligand. Strong N coordination (modes **4** and **5**) results in a decrease in the $-NO_2$ stretching frequency. $\nu_{as}(NO_2)$ is also decreased with strong N, weak O coordination (mode **1**), but not to the extent observed for bonding modes **4** or **5**.

Acknowledgment. We are grateful to Morton-Thiokol, Inc., for support for this work on an Independent Research and Development Program. We thank Drs. David A. Flanigan, Winston Brundige, Ernest Sutton, and Rodney Willer for valuable discussions during the course of this work.

(28) Atkinson, G.; Bauman, J. E., Jr. *Inorg. Chem.* **1963**, *2*, 67.
(29) Kepert, D. L. *Prog. Inorg. Chem.* **1977**, *23*, 1. Normalized bite is defined as the distance between the donor atoms of the chelate divided by the metal–donor atom distance.
(30) Brill, T. B.; Oyumi, Y. *J. Phys. Chem.* **1986**, *90*, 2679.
(31) Nakamoto, K. *Infrared Spectra of Inorganic and Coordination Compounds*; Wiley: New York, 1970; p 162.

Supplementary Material Available: Listings of anisotropic thermal parameters (Tables 1S, 4S, 7S, 10S, 13S, 16S, and 19S) and hydrogen atom coordinates (Tables 2S, 5S, 8S, 11S, 14S, 17S, and 20S) for I-VII and bond distances and angles for V (Tables S22, S23) and crystal packing diagrams for I-VII (Figures S1-S7) (18 pages); listings of observed and calculated structure factors (Tables 3S, 6S, 9S, 12S, 15S, 18S, and 21S) for I-VII (71 pages). Ordering information is given on any current masthead page.

Contribution from the Department of Chemistry,
University of Delaware, Newark, Delaware 19716

Thermal Decomposition of Energetic Materials. 30. Thermolysis of Energetic Metal-Nitraminato Complexes under Conditions That Simulate Combustion

S. F. Palopoli and T. B. Brill*

Received February 3, 1988

The thermal decomposition of six energetic nitraminato complexes of Cu(II), Pd(II) and Ni(II) was investigated at 5 °C/min by IR spectroscopy and DSC and at 100 °C/s (to simulate combustion) by rapid-scan infrared spectroscopy. The objective was to correlate, insofar as possible, the structure and bonding of the parent complex to the decomposition behavior and products. The metal-nitraminato complexes decompose very rapidly. The gases liberated are farther along toward final combustion products than is the case with most organic nitramines subjected to the same thermal conditions. The thermolysis properties of M-$(NH_3)_2[N(NO_2)(CH_2)_2N(NO_2)]$ (M = Cu, Pd) complexes can be understood in terms of the relative strengths of the metal-nitrogen bond. Most of the NH_3 is retained by the Pd complex in the condensed phase while decomposition occurs, whereas more of the NH_3 is released to the gas phase in advance of decomposition by the Cu complex. There is circumstantial evidence that the high potential for forming $^{\bullet}H$ in the ammine complexes drives the thermolysis farther along toward the final, thermodynamically stable products. The Ni(II) complexes were more difficult to characterize because the thermal stimulus exploded the samples.

Introduction

The objective of this research program has been to uncover relationships between the bonding and molecular structure of selected molecules and the distribution of gas products evolved under conditions that simulate ignition and combustion. New thermolysis techniques have been developed for this work that employ rapid-scanning infrared spectroscopy as the principal analytical tool.[1,2] The experiments are designed to give a phenomenological understanding of thermolysis mechanisms as opposed to kinetic data. This is because the processes taking place are multistep, physicochemical in nature, and nonisothermal and involve the heterogeneous gas and condensed phase. Despite the complexity of the events and the experimental trade-offs that studies of this type require, much new insight has been achieved. This program has been directed mainly at energetic organic molecules containing N-NO_2,[1,3-15] O-NO_2,[16] and C-NO_2[3,5,6,17-20] linkages: azides,[1,2,15,21] furazans,[22] furoxans,[8] nitrate salts,[20,23,25] and perchlorate salts.[24] Some guidelines have emerged on the factors influencing the tendency of these compounds to liberate NO_2,[7,10] HONO,[9] N_2O,[6,13] NO,[9] HNO_3,[20,23-25] CH_2O,[6,13] NH_3,[20] and CH_4[21] upon high rate thermolysis. The influence of cyclization of linear nitramines on the thermolysis[11] and condensed-phase[26] properties was analyzed. Some of the chemistry that occurs when decomposition transits to deflagration was captured in real time in the same experiment.[18] The effect of pressure on identity of the first observed gas products was analyzed.[27]

Successful studies of this type require rapid, real-time measurements because the gas products are often quite reactive. If certain products are missed, then the relationship between the observed gas products and the structure and bonding of the parent molecule may not be decipherable. Even with all of these precautions taken into account, only a few of the products come from primary decomposition reactions. On the other hand, the species have sufficient stability to exist in concentrations to control the various flames of a combusting material. These products thus strongly influence the combustion properties. Given the complexity of the decomposition/ignition/combustion process, the conclusions that can be drawn from our studies are largely qualitative. However, they present new insights into the thermal degradation reactions of materials under conditions that approach combustion.

This paper describes the first real-time, in situ, gas product speciation studies of metal complexes subjected to high heating rates and pressures. Our objective was to uncover some of the relationships between the structure and bonding in the parent energetic metal complexes and their decomposition products. Both slow and fast thermolysis experiments were conducted. The compounds investigated are the metal-nitraminato complexes whose syntheses and structures are described in the preceding paper in this issue. Some of these compounds might be potentially

(1) Oyumi, Y.; Brill, T. B. *Combust. Flame* **1985**, *62*, 213.
(2) Cronin, J. T.; Brill, T. B. *Appl. Spectrosc.* **1987**, *41*, 1147.
(3) Oyumi, Y.; Brill, T. B. *Combust. Flame* **1985**, *62*, 225.
(4) Oyumi, Y.; Brill, T. B. *Combust. Flame* **1985**, *62*, 233.
(5) Oyumi, Y.; Brill, T. B.; Rheingold, A. L. *J. Phys. Chem.* **1985**, *89*, 4824.
(6) Oyumi, Y.; Rheingold, A. L.; Brill, T. B. *J. Phys. Chem.* **1986**, *90*, 2526.
(7) Brill, T. B.; Oyumi, Y. *J. Phys. Chem.* **1986**, *90*, 2679.
(8) Oyumi, Y.; Rheingold, A. L.; Brill, T. B. *J. Phys. Chem.* **1986**, *90*, 4686.
(9) Brill, T. B.; Oyumi, Y. *J. Phys. Chem.* **1986**, *90*, 6848.
(10) Oyumi, Y.; Rheingold, A. L.; Brill, T. B. *Propellants Explos. Pyrotech.* **1987**, *12*, 1.
(11) Oyumi, Y.; Brill, T. B.; Rheingold, A. L. *Thermochim. Acta* **1987**, *114*, 209.
(12) Oyumi, Y.; Rheingold, A. L.; Brill, T. B. *J. Phys. Chem.* **1987**, *91*, 920.
(13) Oyumi, Y.; Brill, T. B. *Combust. Flame* **1987**, *67*, 121.
(14) Palopoli, S. F.; Brill, T. B. *Combust. Flame* **1988**, *72*, 153.
(15) Brill, T. B.; Karpowicz, R. J.; Haller, T. M.; Rheingold, A. L. *J. Phys. Chem.* **1984**, *88*, 4139.
(16) Oyumi, Y.; Brill, T. B. *Combust. Flame* **1986**, *66*, 9.
(17) Oyumi, Y.; Brill, T. B. *Combust. Flame* **1986**, *65*, 103.
(18) Oyumi, Y.; Brill, T. B. *Propellants Explos. Pyrotech.* **1986**, *11*, 35.
(19) Oyumi, Y.; Rheingold, A. L.; Brill, T. B. *Propellants Explos. Pyrotech.* **1987**, *12*, 46.
(20) Oyumi, Y.; Brill, T. B. *J. Phys. Chem.* **1987**, *91*, 3657.
(21) Oyumi, Y.; Brill, T. B. *Combust. Flame* **1986**, *65*, 127.
(22) Oyumi, Y.; Brill, T. B. *Combust. Flame* **1986**, *65*, 313.
(23) Oyumi, Y.; Brill, T. B.; Rheingold, A. L.; Lowe-Ma, C. *J. Phys. Chem.* **1985**, *89*, 2309.
(24) Oyumi, Y.; Brill, T. B. *J. Phys. Chem.* **1985**, *89*, 4325.
(25) Cronin, J. T.; Brill, T. B. *J. Phys. Chem.* **1986**, *90*, 178.
(26) Oyumi, Y.; Brill, T. B. *Thermochim. Acta* **1987**, *116*, 125.
(27) Oyumi, Y.; Brill, T. B. *Combust. Flame* **1987**, *68*, 209.

0020-1669/88/1327-2971$01.50/0 © 1988 American Chemical Society